<u>Self-Powered Wireless Sensor Module</u>

Submitted by Eu Jin Ooi on 9 September 2013

Supervised by Ridha Ben Mrad

1. Introduction

A self-powered wireless sensor module is developed in this project. The module will periodically enter an operational mode where it gathers data from its sensors, and then transmit the data to a receiver via its wireless module. While not operating, it will be put on standby mode to reduce power consumption. It will be powered by a piezoceramic energy harvester which gathers and stores energy through motion (humans, vehicles and wind).

It is made up of two main components, i.e., the loading unit and the supply unit. The loading unit consists of a microcontroller, sensors and a wireless module for data transmission. The supply unit primarily consists of a piezoceramic energy harvester and its conditioning circuitry.

2. Objectives

The wireless sensor module should meet the following objectives:

1. Reliable: Long product lifetime
2. Portable: Small and light
3. Durable: Should not be affected by wear and tear
4. Long working range of data transmission

3. Applications

The self-powered module can be applied for various applications based on the type of sensors used. This technology can be applied in three main fields: structural health monitoring, human tracking and animal tracking.

4. Electrical Design

The wireless sensor module is divided into two main components:

1. Loading unit: microcontroller, sensors, wireless module
2. Supply unit: piezoceramic energy harvester, conditioning circuitry

In this section, the designs for both units are discussed. At the end of this section, printed circuit board (PCB) designs used to miniaturize the modules are shown.

4.1. Loading Unit

For the loading unit, two designs were developed. Design 1 integrates off-the-shelf electronics to demonstrate the ability to produce a wireless sensor module. Design 2 integrates low power electronics to allow the module to be self-powered.

4.1.1. Design 1: Off-the-shelf Electronics

Off-the-shelf electronics are integrated as a proof-of-concept that an idea of a wireless sensor module is reasonable. The following are the products used:

1. Microcontroller: Arduino Fio board (ATmega328P)

2. Sensors: Infrared thermometer (MLX90614), Pulse sensor
3. Radio module: XBee Series 1 running on IEEE 802.15.4 wireless standard

Initially, the Arduino Uno was used as the microcontroller board due to its simplicity. However, due to its large size and higher power consumption (DC current of 50mA per pin, at an operating voltage of 5V [1]), it is replaced by the Arduino Fio (refer to Figure 1) for Design 1.

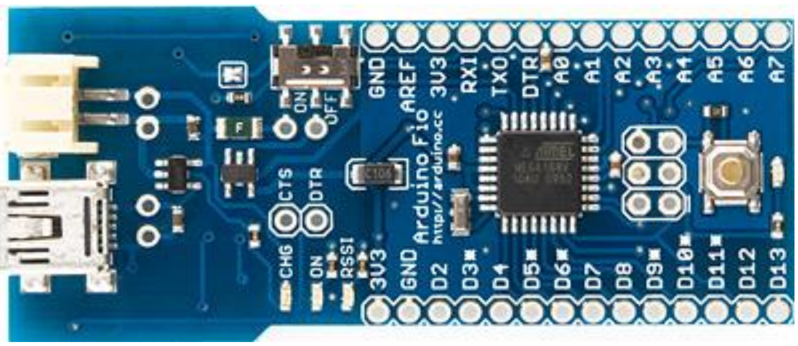

Figure 1: Arduino Fio [2]

Table 1 shows a summary of Arduino Fio's datasheet.

Table 1: Summary of Arduino Fio's datasheet [2]

Microcontroller	ATmega328P
Operating Voltage	3.3V
Input Voltage	3.35 -12 V
Input Voltage for Charge	3.7 - 7 V
Digital I/O Pins	14 (of which 6 provide 8-bit PWM output)
Analog Input Pins	8 (10-bit resolution)
DC Current per I/O Pin	40 mA
Flash Memory	32 KB (of which 2 KB used by bootloader)
SRAM	2 KB
EEPROM	1 KB
Clock Speed	8 MHz

MLX90614 (shown on Figure 2) is a non-contact infrared thermometer which has an internal 17-bit analog-to-digital converter. Inter-integrated circuit (I^2C 2-wire serial bus) is used to communicate between the microcontroller and the MLX90614.

Figure 2: Infrared thermometer [3]

Table 2 shows a summary of MLX90614's datasheet.

Table 2: Summary of MLX90614's datasheet [3]

Thermometer	MLX90614
Supply Voltage	3.6V to 5V
Reverse Voltage	0.4V
Operating Temperature Range	-40℃ to +85℃
DC Operating Current (maximum)	25mA

The pulse sensor (shown on Figure 3) is an open source hardware which is available through Sparkfun. It runs on voltages from 3V to 5V and consumes 4mA at 5V. As an optical pulse sensor, it emits light into a finger tip. The light will then either be reflected by the skin tissues or absorbed by the blood cells. The time between the two occurrences of light absorption is defined as a single heart beat.

Figure 3: Pulse sensor [4]

XBee Series 1 (refer to Figure 4) is a 2.4GHz wireless module with a PCB trace antenna which runs on the IEEE 802.15.4 or ZigBee standard. It has 8 digital input-output pins and 6 10-bit analog-to-digital input pins. The transmitter on the module is made to communicate serially to the receiver on a separate unit at a 57600 baud rate. Table 3 shows a summary of XBee Series 1's datasheet.

Figure 4: XBee Series 1

Table 3: Summary of XBee Series 1

Wireless Module	XBee Series 1
Supply Voltage	3.3V
DC Operating Current	50mA
Data Transmission Range	100m
Power Output	1mW

The design is powered using a 3.7V lithium-ion battery. The microcontroller is programmed using the Arduino Integrated Drive Electronics (IDE) standard which is based on a modified C or “wiring” programming language (part of the code shown on Figure 5). Interrupt service routines are used to enable low power modes and re-activating the module through a microswitch.

```
void loop(){
  if(blinkCount==1){
    //SETUP XBEE
    // Wake up the Xbee. So we can send data to the server
    pinMode(XBEE_sleepPin,OUTPUT);    // Set the "wake-up pin" t
    digitalWrite(XBEE_sleepPin,LOW); // wake-up XBee
    delay(1000);
    // Start serial communication
    // Set up the searial port
    Serial.begin(57600);
    Serial.println("Setup...");

    //CALL TEMPERATURE
    for(i=0;i<5;i++){
      sumTemp+=temp();
    }
    Serial.print("Celcius: ");
    Serial.println(sumTemp/5);
    sumTemp=0;

    //CALL PULSE
    while(countInt<=10){
    pulse();
    delay(2);
    }
    Serial.println(BPM);
    countInt=0;

    blinkCount=0;
  }
  delay(500);      // wait a bit to ensure the data was sent vi
  sleepNow();      // sleep function called here
}
```

Figure 5: Part of the code used for Design 1

The logic used in programming the microcontroller for Design 1 is shown on Figure 6.

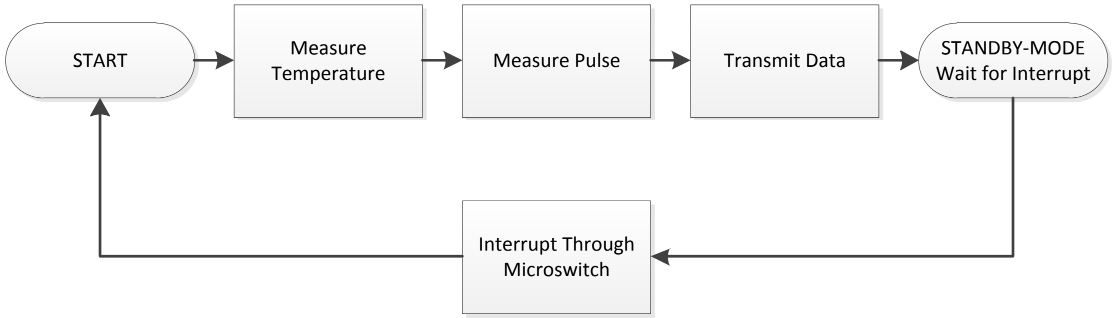

Figure 6: Flow chart for Design 1 programming logic

Based on the power requirement tests, it is determined that the loading circuit powered by the 3.7V lithium-ion battery consumes 3.1mA (11.47mW) on standby mode and 64.6mA (239.02mW) on operational mode (shown on Figure 7).

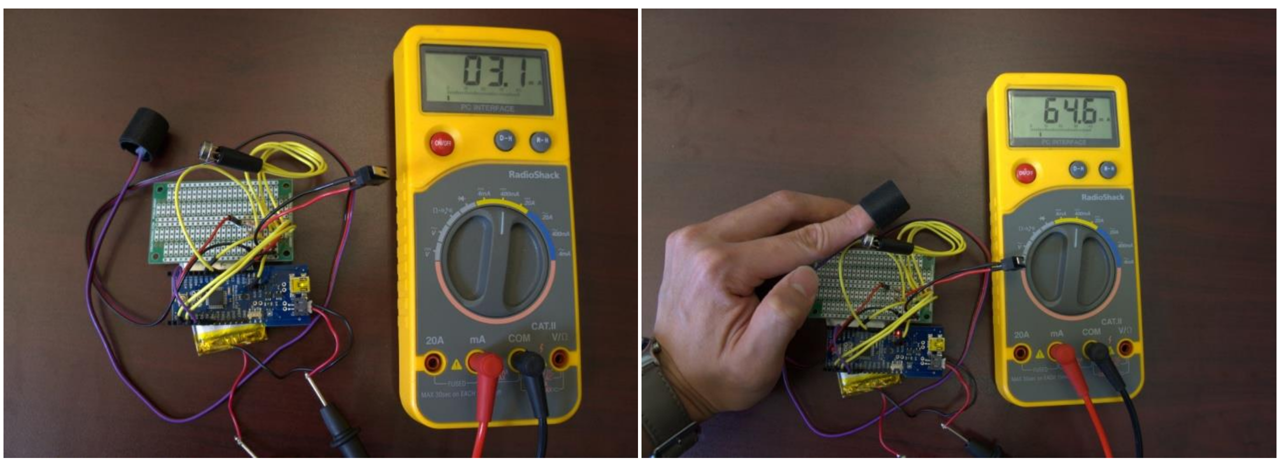

Figure 7: Power requirement tests (left: standby mode, right: operational mode)

The current state-of-the-art piezoceramic energy harvester is capable of generating 100μW from a body vibrating at a constant 1g or 9.81m/s^2 acceleration. Since power consumption by this design cannot be sustained by the energy harvester, it is required to seek low-power electronics.

4.1.2. Design 2: Low-power Electronics

Based on the issues faced in Design 1, it is required for Design 2 to consume less power in order to meet the capabilities of the piezoceramic energy harvester. The frequency of data transmission by the module will be governed by the ratio of power consumptions during operational mode and during standby mode.

The low-power microcontrollers and radio frequency modules available in the market are shown on Table 4 and Table 5.

Table 4: Low-power microcontrollers

Company	Part Number	Flash (kB)	I/O ports	Operating Power (mW)	Shut-down Power (uW)
Texas Instruments	MSP430G2	16	16	1.386	1.65
Microchip	PIC12F1822	8	11	1.728	0.036
ST Microelectronics	STM8L101	8	30	2.31	1.155
Lapis Semiconductor	ML610Q421	32	22	8.25	1.65
Silicon Labs	C8051F91	16	16	12.9	1.98

Table 5: Low-power radio frequency modules

Company	Part Number	Frequency	Range	Operating Power (mW)	Shut-down Power (uW)
Linx Technologies	LR Series	433MHz	1km	5.94	16.5
RF Monolithics	TRC104	2.4GHz	<100m	27	1.32
Semtech	SX1240	434/868MHz	n/a	29.7	3.3
RF Monolithics	XDM2140	2.4GHz	<100m	54	28
RF Solutions	TRX433	434/868/915	n/a	42.9	0.99

Current state-of-the-art low-power sensors are also looked into to improve the module's feasibility, as shown on Table 6 to Table 9.

Table 6: Low-power thermometers

Company	Part Number	Output (bits)	Measurement Range (C)	Accuracy	Operating Power (uW)	Shut-down Power (uW)
Texas Instruments	TMP20	Analog	-55 to 130	2.5	19.8	0.066
ST Microelectronics	STLM20	Analog	-55 to 130	1.5	26.4	0.066
Microchip	MCP9700	Analog	-40 to 150	2	39.6	n/a
ST Microelectronics	STTS75	Digital (9 to 12)	-55 to 125	0.5	330	3.3
Texas Instruments	TMP006	Digital (16)	-40 to 125	n/a	1070	3.3

Table 7: Low-power accelerometers

Company	Part Number	# of Axis	Measurement Range (g)	Sensitivity (mg/LSB)	Operating Power (uW)	Shut-down Power (uW)
Analog Devices	ADXL362	3	2/4/8	1/2/4	5.9	0.033
Kionix	KX023	3	2/4/8	1/2/4	33	6.6
ST Microelectronics	LIS3DH	3	2/4/8/16	1/2/4/12	36.3	1.65
Freescale	MMA8450Q	3	2/4/8	1/2/4	138.6	3.3

Note: Data is for 50Hz operation

Table 8: Low-power gyroscope

Company	Part Number	# of Axis	Measurement Range (dps)	Sensitivity (mdps/LSB)	Operating Power (mW)	Shut-down Power (mW)
Maxim Integrated	MAX21000	3	500/1000/2000	16.7/33.3/66.7	17.82	0.028
InvenSense	MPU3000	3	250/500/1000/2000	7.6/15.0/30.5/61.0	20.13	0.0165
ST Microelectronics	L3G4200D	3	250/500/2000	8.75/17.5/70	20.13	0.0165
Analog Devices	ADXRS450	1	300	12.5	33	n/a
Analog Devices	ADIS16260	1	80/160/320	18.3/36.6/73.3	135.3	1.16

Note: dps: degrees/second; LSB: least significant bit

Table 9: Low-power GPS

Company	Part Number	Horizontal Accuracy 90% (m)	Altitude Accuracy 90% (m)	Operating Power (mW)	Shut-down Power (mW)
Fastrax	IT430	n/a	n/a	68	0.036
Trimble	Copernicus 2	4	5	132	0.0396
Trimble	Lassen LP	9	18	221	24

The microcontroller, radio frequency module and sensors with the lowest operating power consumptions are chosen for Design 2. Thermometers and accelerometers are chosen to be integrated due to their relatively lower power consumptions compared to the other sensors. The theoretical total power consumption by Design 2, integrating the chosen electronics is shown on Table 10.

Table 10: Total power consumption by Design 2

Component	Company	Operating Power	Standby Power
Microcontroller	Texas Instruments	1.386mW	1.65μW
Thermometer	Texas Instruments	19.8μW	0.066μW
Accelerometer	Analog Devices	5.9μW	0.033μW
RF module (Transmitter)	Linx Technologies	5.94mW	16.5μW
Total		**7.3517mW**	**18.249μW**

MSP430 Texas LaunchPad (refer to Figure 8) is used as the microcontroller board for prototyping development purpose. The microcontroller (MSP430G2553) is programmed using this board via USB serial communication.

Figure 8: MSP430 Texas LaunchPad [5]

MSP430G2553 is programmed using the Energia IDE, which is based on modified C or "wiring" language (part of the code shown on Figure 9). Testing and evaluation of the program can be done on the board itself which consists of voltage regulators, jumpers and male headers directly connected to the pins of the microcontroller. The programmed microcontroller can then be removed and plugged into a breadboard for further development. It is important to note that pin XIN is programmed to be HIGH while pin XOUT is programmed to be LOW during operational mode. These two pins are then used to provide power supply to the sensors and radio modules.

The microcontroller is initially integrated with the sensors, i.e., TMP20 which measures temperature through contact and ADXL362 which measures tri-axial acceleration. Since TMP20 is a surface mount device (SMD), a breakout board is fabricated to enable prototyping using the breadboard. Since breakout boards for ADXL362 are available in the market, additional fabrication for this device is not required.

ADXL362 (refer to Figure 10) is a 12-bit digital accelerometer which communicates with the microcontroller via the Serial Peripheral Interface (SPI) method. Using the SPI command, the range of ±2g is chosen for this application. It has a wide operating voltage range of 1.6V to 3.5V. The pin connections from the breakout board to the microcontroller are shown on Table 11.

```
void loop()
{
  longdelay(10);

  //Data[] is registered
  sensors_begin();
  accelerometer();
  thermometer();

  Serial.println();
  Serial.println();
  Serial.println();

  //SingleData[] is registered
  int i;
  SDCounter=0;
  for(i=0;i<4;i++){
    dataPrep(data[i]);
  }

  bitCounter=0;
  int j, proto=0;

  //Bits[] is registered
  SDCounter=0;
  for(j=0;j<4;j++){
    bits[bitCounter++]=(proto++)%2; //first protocol bit (alternating 1 and 0)
    dataRecog(j); //three bits for data recognition (0: XData, 1: YData, 2: ZData, 3: Temperature)
    bits[bitCounter++]=singleData[SDCounter++]; //positive/negative bit
    for(i=0;i<4;i++){
      bits[bitCounter++]=(proto++)%2;
      dataRecog(j);
      bitPrep(singleData[SDCounter++]); //four bits for each data digit
    }
  }
```

Figure 9: Part of the code used for Design 2

Figure 10: Digital accelerometer, ADXL362 [6]

Table 11: Pin connections from ADXL362 to MSP430G2553

ADXL362	**MSP430G2553**
SCK	Pin 1.5
MOSI	Pin 1.7
MISO	Pin 1.6
CS	Pin 1.0
V+	XIN
GND	XOUT

TMP20 (refer to Figure 11) is a precision analog output temperature sensor which operates from -55℃ to +130℃ on a supply voltage of 2.7V to 5.5V. The pin connections from the breakout board of TMP20 to the microcontroller are shown on Table 12.

Figure 11: Analog temperature sensor, TMP20

Table 12: Pin connections from TMP20 to MSP430G2553

TMP20	**MSP430G2553**
Analog VOut	Pin 1.1
V+	XIN
GND (2)	XOUT

The Linx Technologies LR Series Basic Evaluation kit (refer to Figure 12) is used to integrate the radio module into Design 2. The kit includes a receiver module and a transmitter module. The transmitter module is powered externally via the XIN and XOUT pins on the microcontroller. The receiver module is also powered externally via another MSP430G2553 microcontroller to allow serial communication with the computer through the USB port. Theoretically, the two modules are able to communicate up to a range of 1km. The antennas included are external 433MHz antennas. The modules communicate via 8 digital bits (or 1 byte). The pin connections from the transmitter module to the microcontroller are shown on Table 13.

Figure 12: LR Series Basic Evaluation kit [7]

Table 13: Pin connections from LR Series transmitter to MSP430G2553

LR Series transmitter	**MSP430G2553**
VCC	XIN
GND	XOUT
D0 – D5	Pin 2.0 – Pin 2.5
D6	Pin 1.3
D7	Pin 1.4

The 8 bits are utilized as shown on Table 14.

Table 14: 8-bit utilization

0	1	2	3	4	5	6	7
Alternate	Data Recognition			Single decimal digit of data			

A protocol is designed to ensure that the data transmitted is received correctly by the receiver. 4 bits (0, 1, 2 and 3) are used for this purpose. The first bit (Bit 0) will be alternately written 0 and 1 for subsequent data transmissions. Bits 1, 2, 3 are used to store binary digits converted from decimal digits used for data recognition shown on Table 15.

Table 15: Data recognition bits

Decimal Digit	Binary Digits	Representation
0	000	X-axis acceleration
1	001	Y-axis acceleration
2	010	Z-axis acceleration
3	011	Temperature

The transmitter transmits 4 data, i.e., accelerations in the X, Y and Z axes, and temperature. Acceleration data have 4 decimal digits since the accelerometer have a 12-bit output resolution (2^0 to $2^{12} \rightarrow$ 0 to 4096). Similarly, the temperature data have 4 decimal digits because TMP20's analog output is fed into MSP430G2553 microcontroller which uses a 10-bit analog-to-digital converter for its Input/Output (I/O) pins (2^0 to $2^{10} \rightarrow$ 0 to 1024). A single decimal digit requires 4 bits for binary representation; thus, Bits 4 to 7 are used for this purpose.

In the first byte of a data, Bit 4 will be used to transmit the sign of the data, i.e., 1 for positive and 0 for negative. Table 16 shows an example of the 4 distinct data being represented by 20 bytes.

Table 16: An example of the 8-bit representation of the data

Raw Data	Represent	*Alternate*	*Data Representation*			*Single Decimal Digit*			
		Bit 0	**Bit 1**	**Bit 2**	**Bit 3**	**Bit 4**	**Bit 5**	**Bit 6**	**Bit 7**
X-axis acceleration -0656	Negative	0	0	0	0	0			
	0	1	0	0	0	0	0	0	0
	6	0	0	0	0	0	1	1	0
	5	1	0	0	0	0	1	0	1
	6	0	0	0	0	0	1	1	0
Y-axis acceleration -0077	Negative	1	0	0	1	0			
	0	0	0	0	1	0	0	0	0
	0	1	0	0	1	0	0	0	0
	7	0	0	0	1	0	1	1	1
	7	1	0	0	1	0	1	1	1
Z-axis acceleration +1127	Positive	0	0	1	0	1			
	1	1	0	1	0	0	0	0	1
	1	0	0	1	0	0	0	0	1
	2	1	0	1	0	0	0	1	0
	7	0	0	1	0	0	1	1	1
Temperature +0388	Positive	1	0	1	1	1			
	0	0	0	1	1	0	0	0	0
	3	1	0	1	1	0	0	1	1
	8	0	0	1	1	1	0	0	0
	8	1	0	1	1	1	0	0	0

The 4-digit raw data provided in Table 16 requires further representation, in terms of standard SI units. The accelerometer has a range of $\pm$2g and 4096 states present ($2^{\text{number of bits}}=2^{12}$). Since the data provided through the SPI has both positive and negative values, it is assumed that there are 2048 states for both the positive and negative values. Thus, the acceleration resolution is shown as such [8]:

$$Acceleration\ Resolution = \frac{+2\mathrm{g}\ \times\ 9.80665\,\frac{\mathrm{m/s^2}}{\mathrm{g}}}{2048} = 0.0095768\ \mathrm{m/s^2} \qquad \text{[Eq.1]}$$

The acceleration can then be calculated using the following equation.

$$Acceleration = Raw\ Data\ \times 0.0095768\,\mathrm{m/s^2} \qquad \text{[Eq.2]}$$

The microcontroller's I/O pin connecting to the analog output of the thermometer has a range of V_{CC} = 3.7V. Since there are 1024 states present ($2^{\text{number of bits}}=2^{10}$), the voltage resolution of the analog I/O pin is shown as such [8]:

$$Voltage\ Resolution = \frac{3.7V}{1024} = 0.003613V \qquad \text{[Eq.3]}$$

The voltage can then be calculated using the following equation.

$$Voltage\ Output = Raw\ Data\ \times 0.003613V \qquad \text{[Eq.4]}$$

Based on the datasheet for TMP20 [9], the temperature can be calculated using the following equation.

$$Temperature = \frac{Voltage\ Output - 1.8576V}{-11.77mV/℃ \div 1000\,\frac{V}{mV}} \qquad \text{[Eq.5]}$$

The 4-digit data in Table 16, represented in its meaningful standard SI units based on the resolutions calculated in [Eq.1] and [Eq.3] are shown in Table 17.

Table 17: Data represented in standard SI units

Data	**Raw Values**	**SI Units**
X-axis acceleration	-0656	$-0656 \times 0.0095768\mathrm{m}/s^2 = -6.2824\ \mathrm{m}/s^2$
Y-axis acceleration	-0077	$-0077 \times 0.0095768\mathrm{m}/s^2 = -0.73741\ \mathrm{m}/s^2$
Z-axis acceleration	+1127	$+1127 \times 0.0095768\mathrm{m}/s^2 = 10.7931\ \mathrm{m}/s^2$
Temperature	+0388	$[(388 \times 0.003613V) - 1.8576V]/[-0.01177V/℃] = 38.72℃$

The wireless sensor module integrating the MSP430G2553, LR Series radio transmitter, ADXL362 and TMP20 is shown on Figure 13. Figure 14 shows the electrical layout of the receiver component of Design 2.

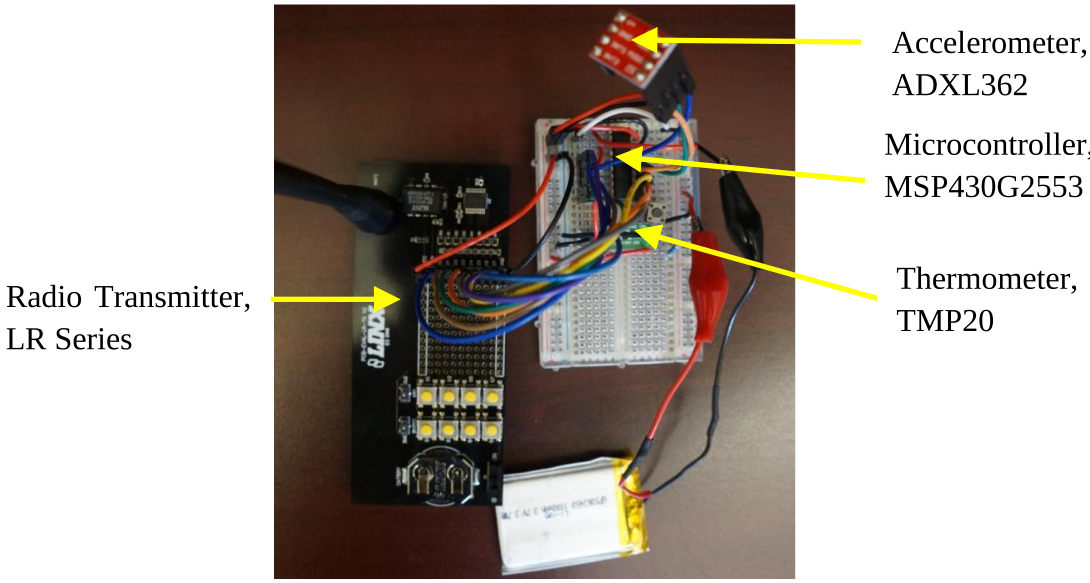

Figure 13: Design 2 module physical layout

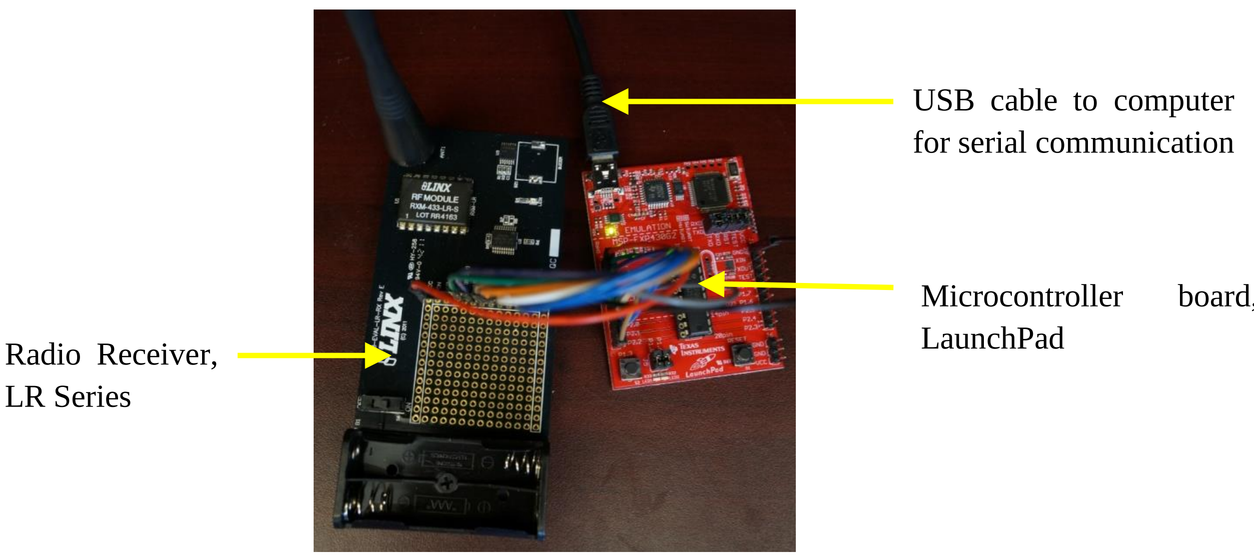

Figure 14: Design 2 receiver unit

The logic implemented in programming the microcontroller for Design 2 is shown on Figure 15.

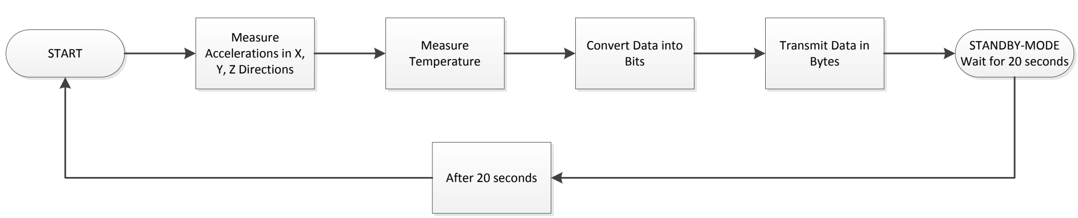

Figure 15: Flow chart for Design 2 programming logic

Since the power consumed by the module is too low to be measured accurately using the ammeter which has the lowest accuracy of $\pm 1\mu A$, it is measured using a low resistance precision resistor (3.6Ω) connected in series to the lithium-ion battery (refer to Figure 16).

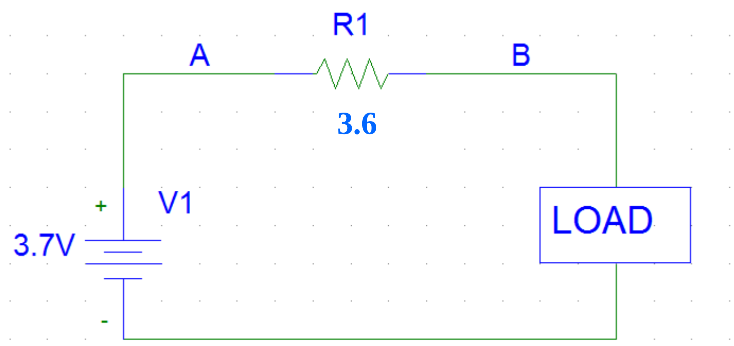

Figure 16: Electrical layout for power requirement tests

The voltage between nodes A and B is measured, and the current flowing from A to B is calculated based on Ohm's law. The power consumed by the entire circuit is then calculated by multiplying 3.7V and the current. Based on the power requirement tests, it is determined that the loading circuit powered by the 3.7V lithium-ion battery consumes $1.944\mu A$ ($7.194\mu W$) on standby mode and 6.944mA (25.694mW) on operational mode. The measured power consumed during standby mode is lower than the theoretical value because all the electrical components except the microcontroller is completely switched off by assigning both XIN and XOUT to LOW values. The microcontroller is also brought to standby mode in this period.

4.2. Supply Unit

The supply unit integrates a piezoceramic energy harvester, a conditioning circuit and an energy storage solution. The energy harvester produces AC supply which is converted to DC supply through the conditioning circuit. The DC supply can then be stored in a lithium-ion battery or in a microsupercapacitor.

4.2.1. Conditioning Circuit

Linear Technology's LTC3588 [10] is the conditioning integrated circuit (IC) used in this unit. The breakout board which connects the IC based on its' user guide is purchased from Sparkfun. The schematic of the breakout board is shown on Figure 17 [11].

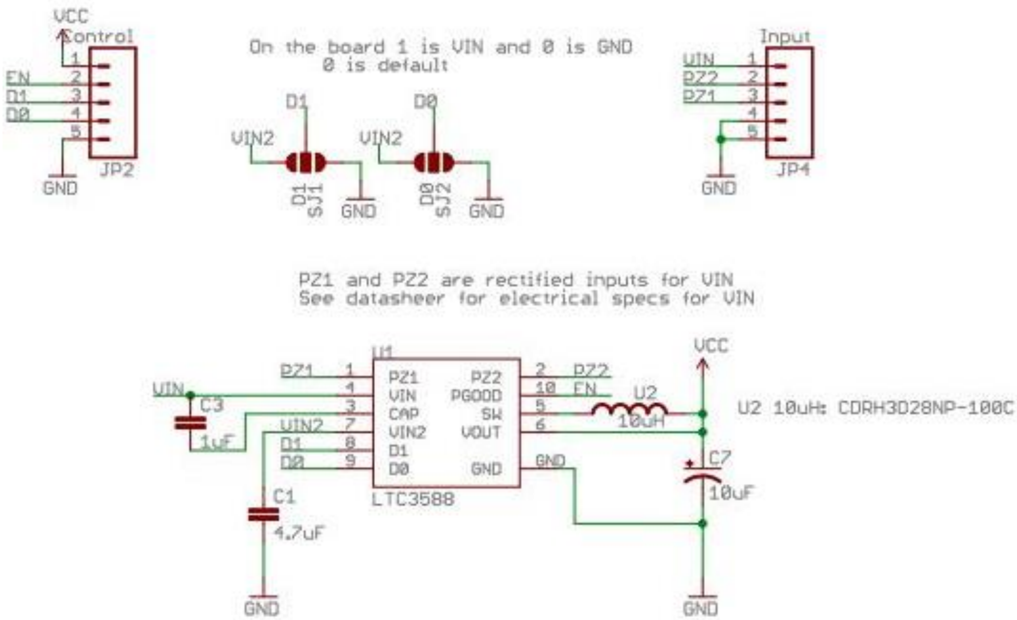

Figure 17: Schematic of LTC3588 breakout board

LTC3588 integrates a full-wave rectifier which ensures the AC supply from the energy harvester is converted to a constant positive polarity supply. It also has a under-voltage lockout (UVLO) circuit which switches on the buck converter when the mean voltage is greater than 5V. The buck converter then transfers the charge from the input capacitor (C3 in Figure 17) to the output capacitor (C7 in Figure 17) by alternating the current passing through the inductor (U2 in Figure 17). A comparator is also present in the IC to compare the output voltage and the target voltage (1.8V, 2.5V, 3.3V, 3.6V). If the output voltage is greater than 92% of the target voltage, pin EN in Figure 17 will produce a HIGH logic output. The flow chart demonstrating the process carried out in LTC3588 is shown on Figure 18.

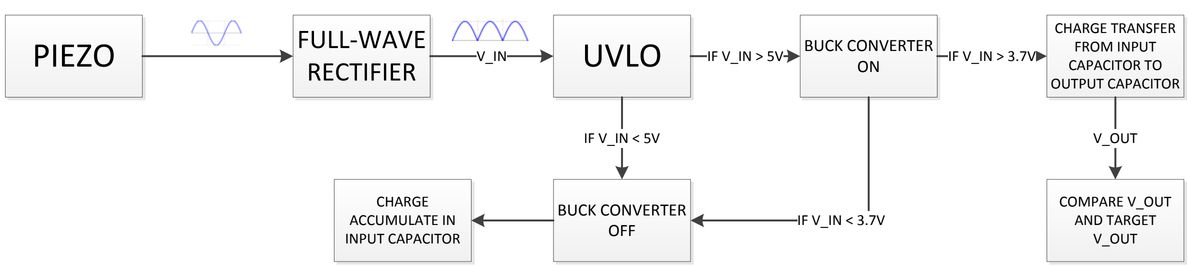

Figure 18: Flow chart demonstrating process in LTC3588

4.2.2. Energy Storage

The DC voltage conditioned by the LTC3588 IC can be stored in a lithium-ion battery or a microsupercapacitor. In this project, the power generated is used to charge a lithium-ion battery. Maxim Integrated's MAX1555 is used as the battery charging IC which directly connects to

LTC3588 (source), and to the lithium-ion battery (load). The pin configuration of MAX1555 is shown on Figure 19.

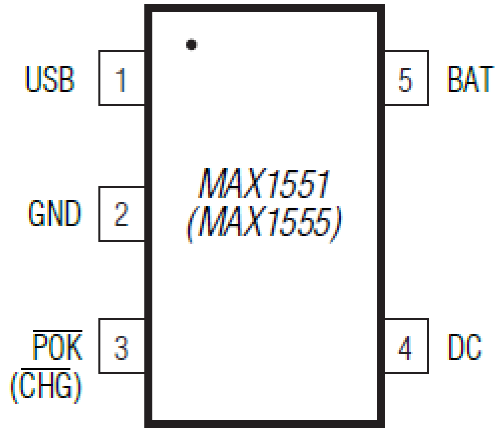

Figure 19: Pin configuration of MAX1555 [12]

Based on MAX1555's datasheet, the minimum voltage which the DC pin must be supplied with is 3.7V. Since V_OUT from LTC3588 can only supply a maximum target voltage of 3.6V, it cannot be used to supply the voltage to the DC pin on MAX1555. Instead, V_IN from LTC3588 can be utilized since it produces a rectified voltage of the energy harvester's AC voltage. The DC pin on MAX1555 has an absolute maximum voltage of 7V. Since the rectified voltage from the energy harvester may reach up to 10V amplitude, a voltage regulator is required. LM317, a 3-terminal adjustable voltage regulator is used. Pin configuration of LM317 is shown on Figure 20.

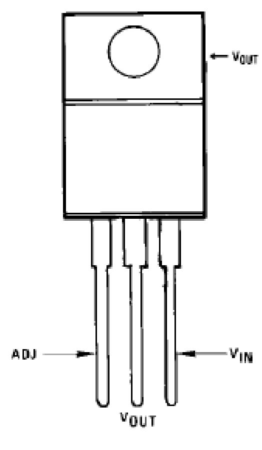

Figure 20: Pin configuration of LM317 [13]

A typical application of LM317 is shown on Figure 21.

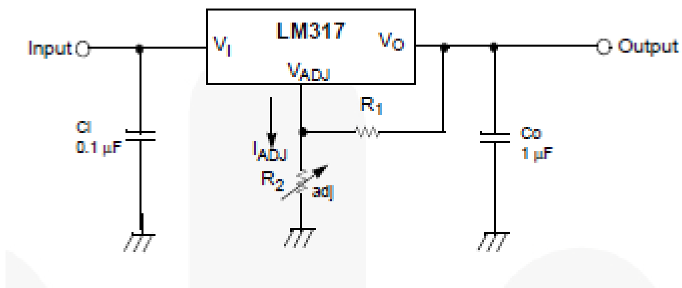

Figure 21: Typical application of LM317 [14]

Based on LM317's datasheet, the output voltage can be computed based on the following equation:

$$V_{output} = 1.25V \times \left(1 + \frac{R_2}{R_1}\right) \quad \text{[Eq.6]}$$

Since it is required for V_{output} to be less than 7V, R_1 is chosen to be 4.7kΩ and R_2 is chosen to be 20kΩ. With this configuration, V_{output} is regulated to 6.569V. The pin connections on LTC3588, MAX1555 and LM317 are shown on Table 18.

Table 18: Pin connections on LTC3588, MAX1555, LM317

LTC3588		**LM317**		**MAX1555**	
PZ1	Piezo +	**V_IN**	V_IN (LTC3588)	**GND**	GND
PZ2	Piezo -	**V_ADJ**	As shown on Figure 21	**DC**	V_OUT (LM317)
GND	GND	**V_OUT**	DC (MAX1555)	**BAT**	V+ (Battery)
V_IN	V_IN (LM317)				

The breadboard which integrates Design 2 with the energy conditioning and energy storage circuitry is shown on Figure 22. The piezoceramic energy harvester is substituted with an AC source which provides a sinusoidal wave of $10V_{pp}$. The frequency is varied from 10Hz to 1MHz to determine the effect of frequency on the circuit. Based on the results, frequency does not significantly affect the circuit's performance.

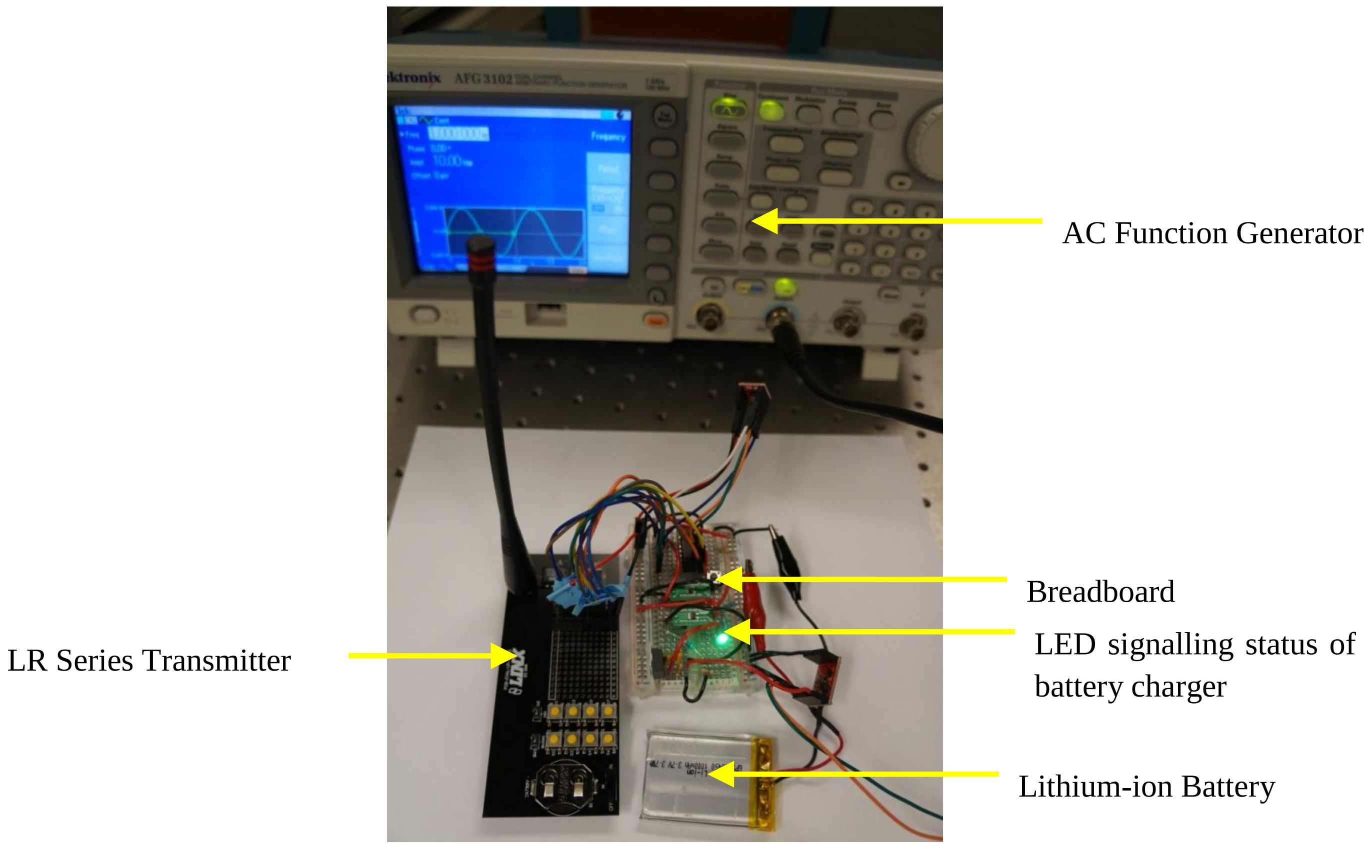

Figure 22: Breadboard layout with AC function generator

4.3. PCB Designs

PCBs are designed to miniaturize both the loading unit and the supply unit, and to integrate both circuits onto a single PCB. The 5 PCBs designed are listed below:

1. WS-Module-rev1.0: Microcontroller and sensors
2. WS-Module-Transmitter: LR Series transmitter and encoder
3. WS-Module-rev1.2: Microcontroller, thermometer, energy harvester conditioning and energy storage
4. WS-Module-rev1.3: Microcontroller, sensors, energy harvester conditioning and energy storage
5. WS-Module-rev1.4: Microcontroller, sensors, energy harvester conditioning, energy storage, and LR Series transmitter and encoder

In order to improve Design 2 (4.1.2), 2 PCBs are designed. The PCB integrating the microcontroller and sensors is named WS-Module-rev1.0 while the PCB which integrates the LR series transmitter and encoder is named WS-Module-Transmitter. It is important to note that WS-Module-rev1.3 integrates all components except the radio module while WS-Module-rev1.4 integrates all the components in both the loading and supply units. The only difference between

WS-Module-rev1.2 and WS-Module-rev1.3 is that WS-Module-rev1.2 is connected externally to the accelerometer ADXL362 breakout board while WS-Module-rev1.3 has the ADXL362 mounted on it.

4.3.1. WS-Module-rev1.0

Schematic for WS-Module-rev1.0 is shown on Figure 23. Capacitors are added into the design to reduce power fluctuations in the circuit. A momentary switch is used as a reset button for the circuit.

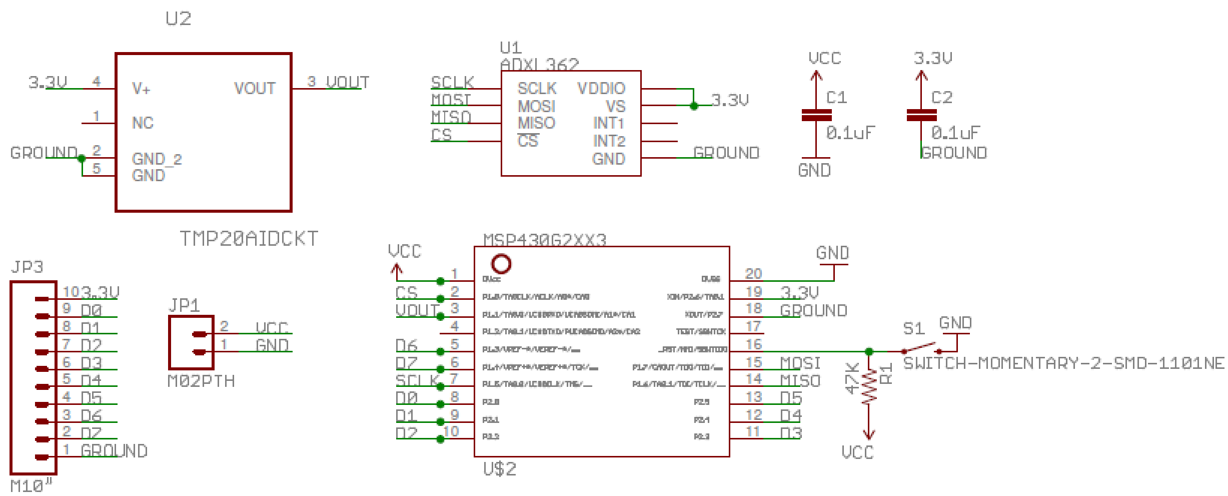

Figure 23: Schematics of WS-Module-rev1.0

The board layout of WS-Module-rev1.0 is shown on Figure 24.

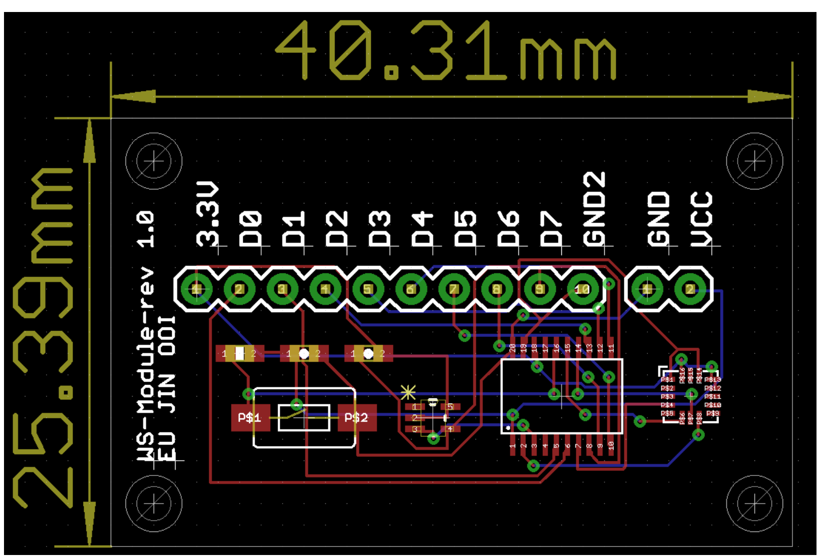

Figure 24: Board layout of WS-Module-rev1.0

The WS-Module-rev1.0 PCB populated with the electronics required is shown on Figure 25.

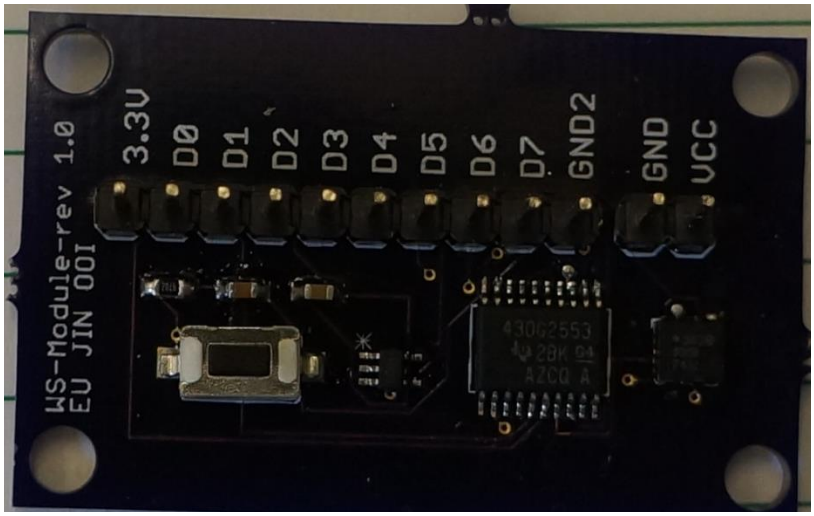

Figure 25: Populated WS-Module-rev1.0 PCB

Electronics are soldered using the hot air reflow technique. The PCB is powered via the GND and VCC header pins and connected to the radio module via the remaining 10 header pins. After carrying out some tests (PCB connected to radio module shown on Figure 26), it is determined that the accelerometer is not functioning on this PCB due to improper soldering technique. The accelerometer is in a quad-flat no-leads (QFN) package which cannot be soldered through regular application of solder paste and hot air reflow technique. Bridges are created through this technique for this particular sensor and cannot be removed using regular solder wick.

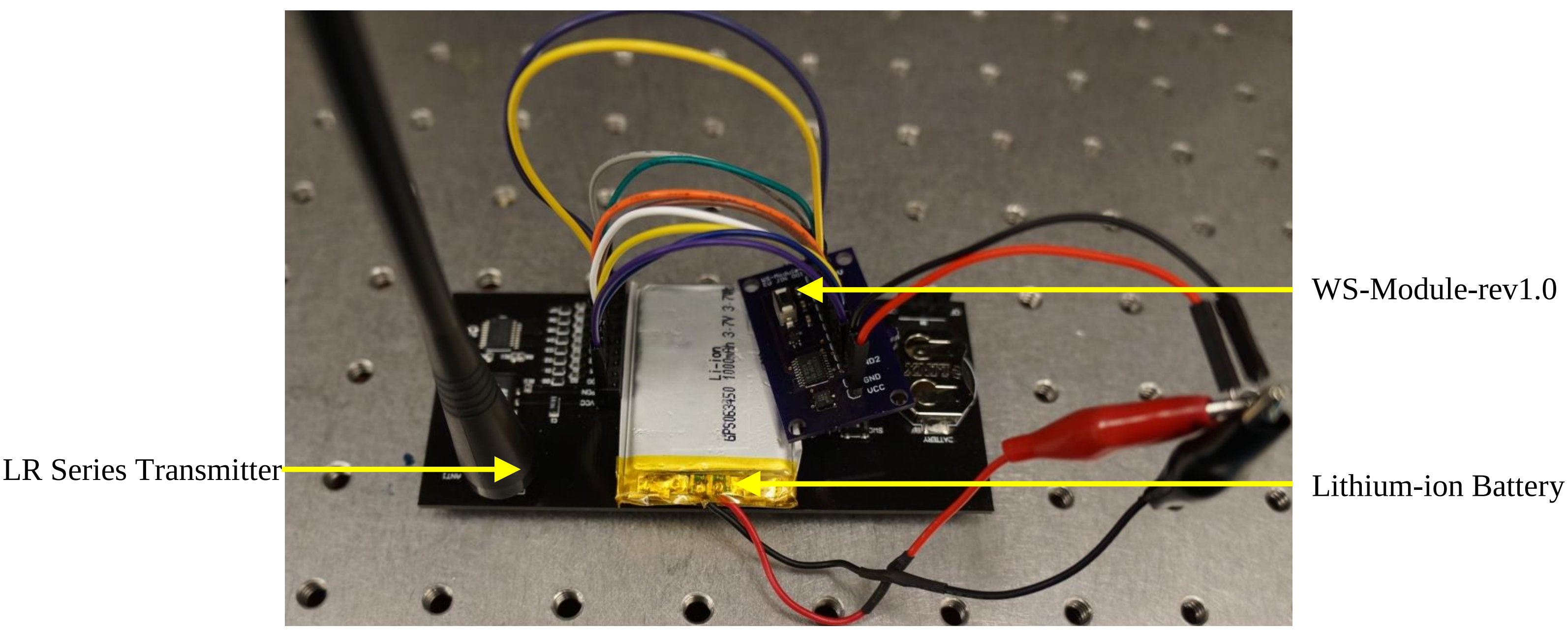

Figure 26: WS-Module-rev1.0 connected externally to radio module

4.3.2. WS-Module-Transmitter

Schematic for WS-Module-Transmitter is shown on Figure 27. The circuit is designed based on the application notes and user guides provided by the manufacturer, Linx Technologies [15]. Jumper wires will be connected from the header pins on WS-Module to the header pins on WS-Module-Transmitter. The board layout of WS-Module-Transmitter is shown on Figure 28.

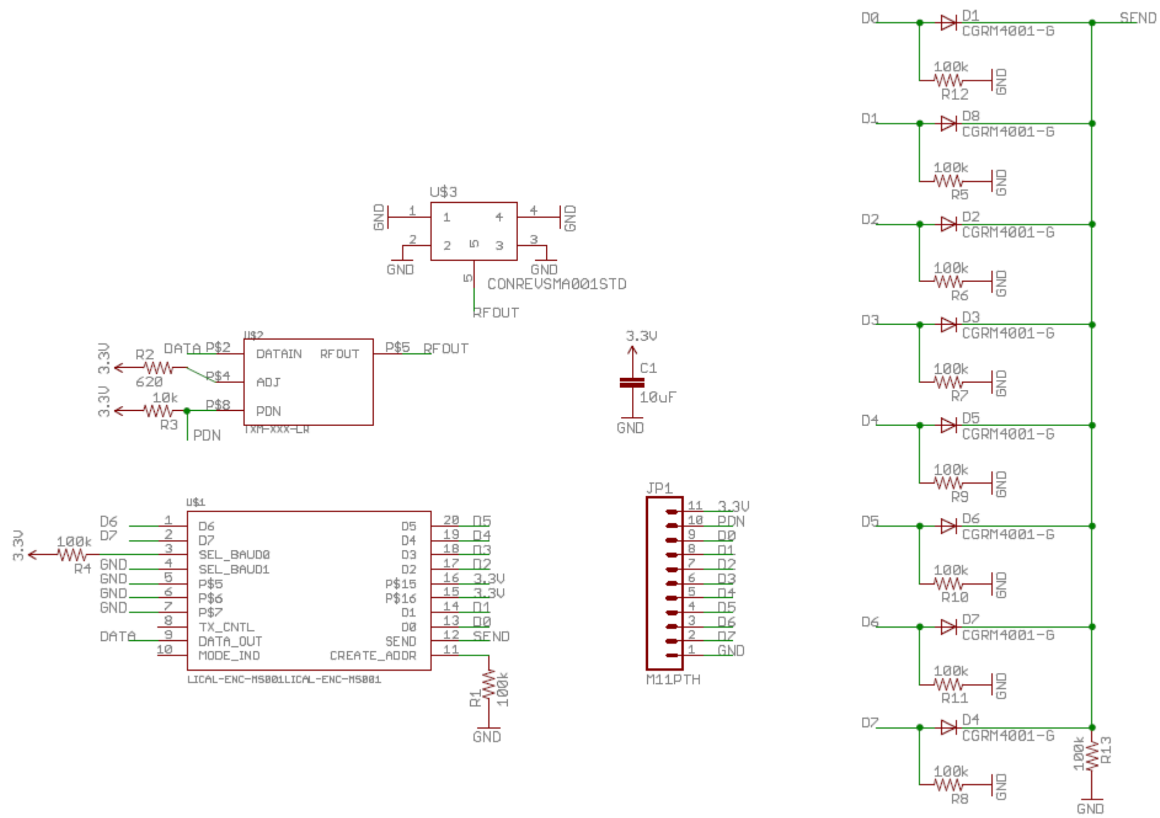

Figure 27: Schematics of WS-Module-Transmitter

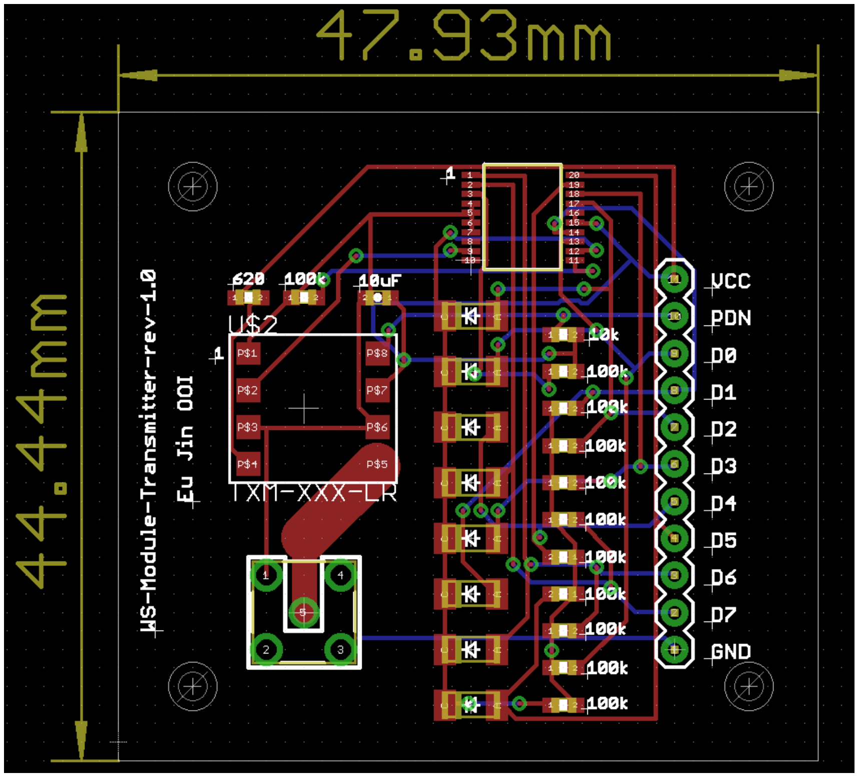

Figure 28: Board layout of WS-Module-Transmitter

In order to improve the radio transmission of data, high power transfer efficiency from the source (LR series transmitter module) to the load (radio antenna) must be achieved. This can be done through impedance matching, i.e., the impedance at the loading unit must be equal to the impedance at the source unit for maximum power transfer. Since the radio antenna has an impedance of 50Ω, the trace from the radio transmitter to the SMA connector (which directly connects to the antenna) must also have an impedance of 50Ω. Figure 29 shows the location of a trace on a standard PCB and the values of variables provided by the PCB manufacturer [16].

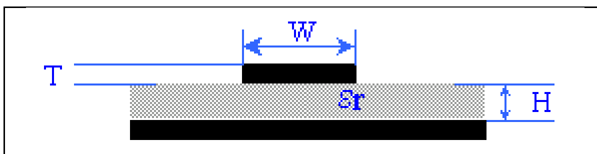

W	Trace width [mm]	**3.21mm**
T	Trace thickness [mm]	0.035mm
H	Dielectric thickness [mm]	1.6mm
ε_r	Relative permittivity	3.7

Figure 29: Trace on a PCB [17]

Using the following formula [18], the trace width required to obtain the 50Ω impedance is 3.21mm.

$$Z_o[\Omega] = \frac{87}{\sqrt{\varepsilon_r + 1.41}} ln \frac{5.98H}{0.8W + T} \quad \text{[Eq.7]}$$

Electronics are soldered onto the PCB using the hot air reflow technique. The PCB is connected to WS-Module-rev10 via header pins. The populated WS-Module-Transmitter PCB connected to the WS-Module-rev10 is shown on Figure 30. After carrying out some tests, it is determined that the transmitter PCB is not functioning. It is deduced that it may be due to incorrect trace width design.

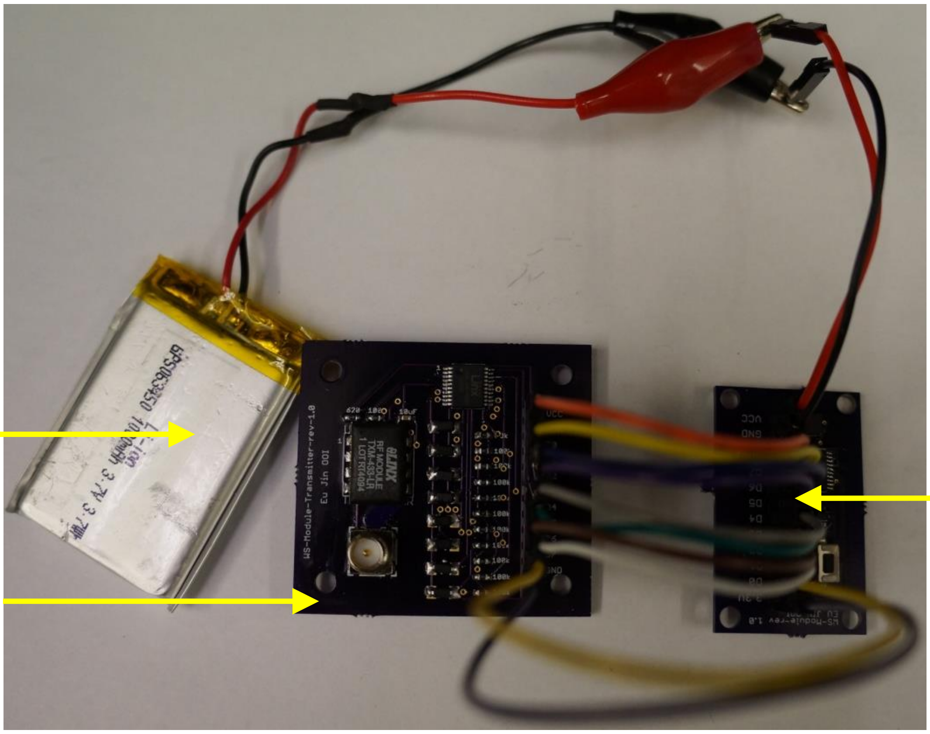

Figure 30: Populated WS-Module Transmitter connected to WS-Module-rev1.0

4.3.3. WS-Module-rev1.2

WS-Module-rev1.2 integrates the microcontroller, thermometer, energy conditioning and energy storage circuitry. The accelerometer ADXL362 breakout board and radio module are then connected externally to this PCB. Schematic of this design is shown in Figure 31.

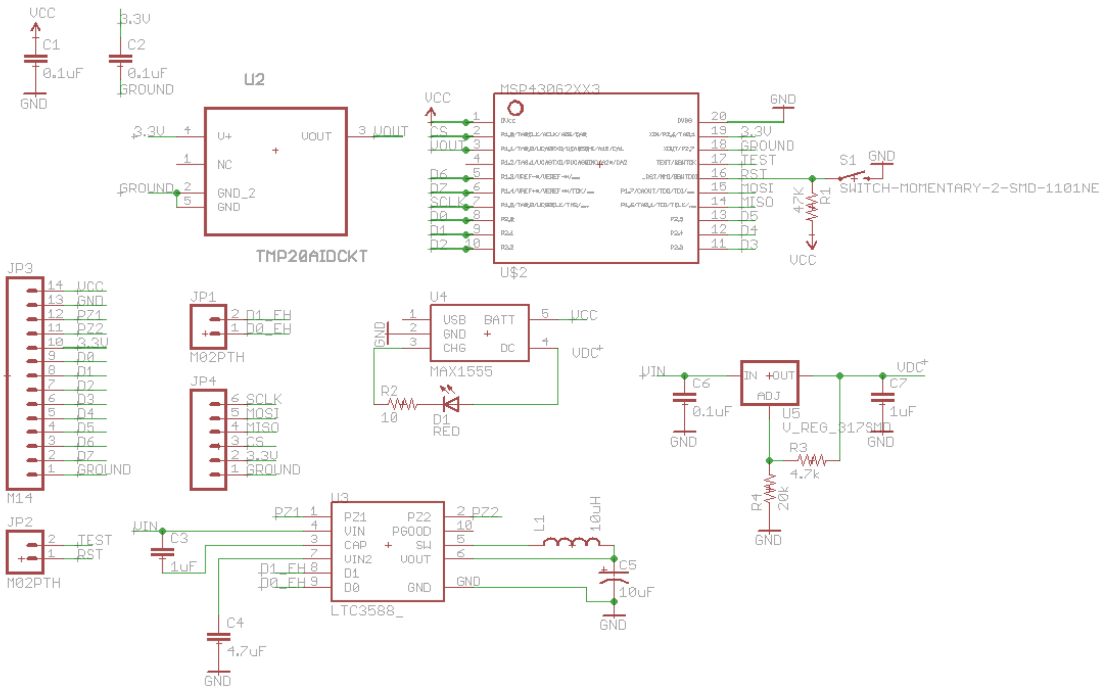

Figure 31: Schematics of WS-Module-rev1.2

The board layout is shown in Figure 32.

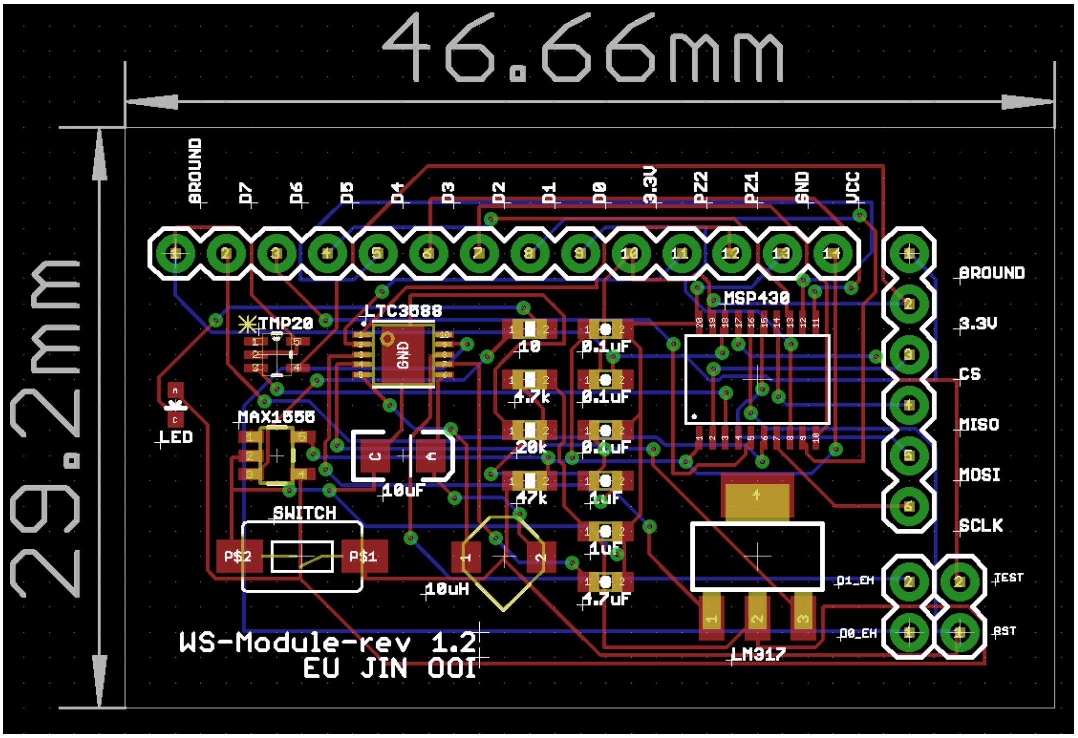

Figure 32: Board layout of WS-Module-rev1.2

Electronics are soldered using the hot air reflow technique. The PCB is connected to the lithium-ion battery, ADXL362 breakout board and radio module via the header pins (shown on Figure 33). The AC source which substitutes the piezoceramic energy harvester is connected to the PCB via pins PZ1 and PZ2. After carrying out tests, it is determined that this PCB design is in working condition.

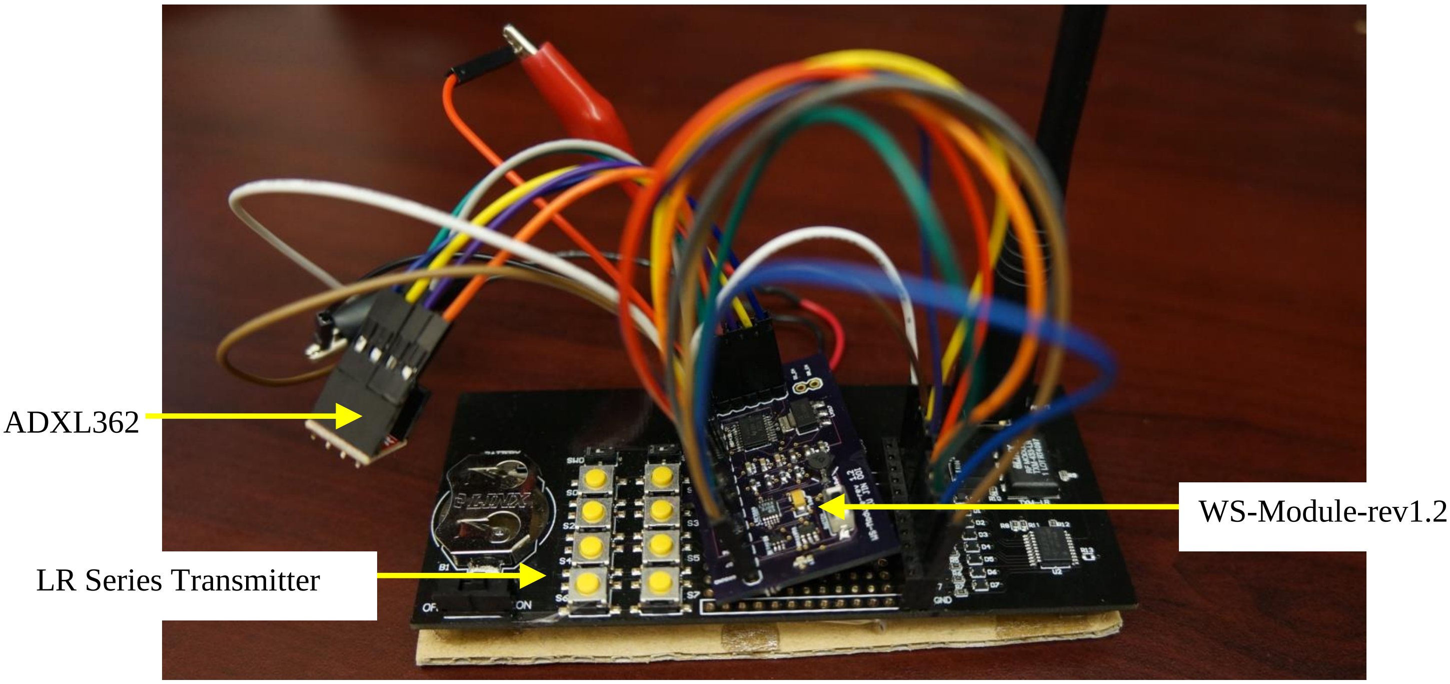

Figure 33: Populated WS-Module-rev1.2 connected to battery, ADXL362 and radio module

4.3.4. WS-Module-rev1.3

WS-Module-rev1.3 integrates the microcontroller, sensors, energy conditioning and energy storage circuitry. The radio module is then connected externally to this PCB to avoid complications. Schematic of this design is shown in Figure 34 and the board layout is shown in Figure 35. Electronics are soldered using the hot air reflow technique. ADXL362 is mounted onto the PCB by applying molten solder onto the PCB pads prior to placing the component. The solder sandwiched between the ADXL362 and pads are then heated up using the hot air reflow gun. Figure 36 shows the populated WS-Module-rev1.3 which is connected to the battery, radio module and AC source. It is important to note that the radio antenna used for this set-up is a surface mount grounded-line planar antenna (SP Series Splatch Antenna by Linx Technologies) instead of the bulky wire antenna. After carrying out tests, it is determined that this PCB design is in working condition.

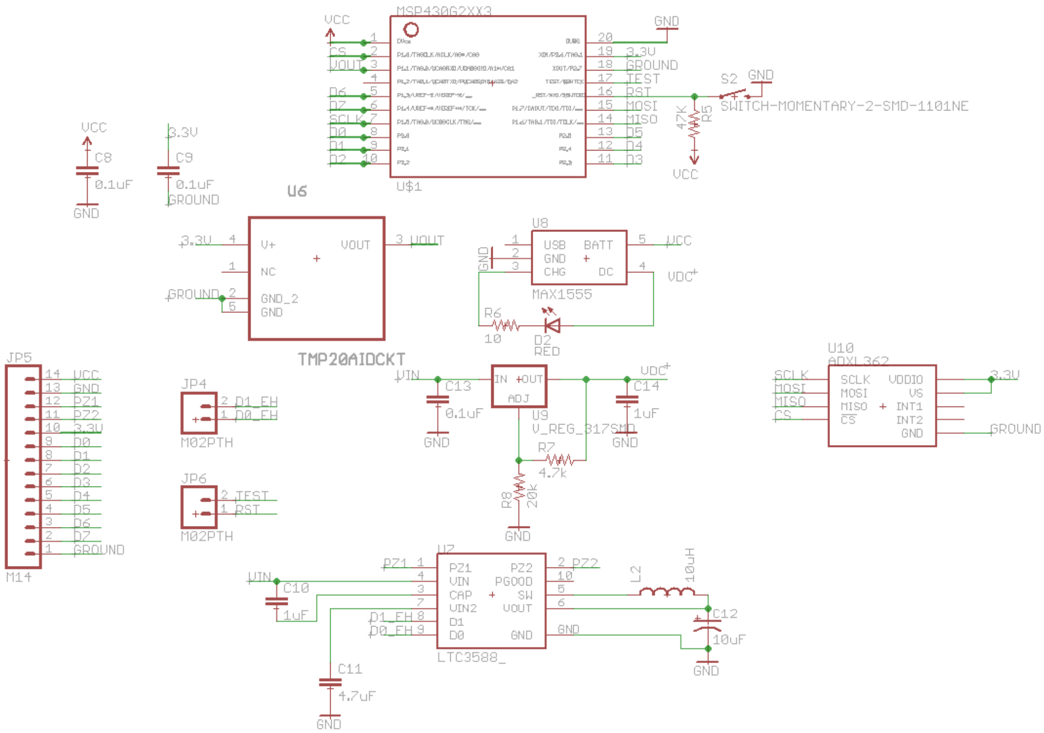

Figure 34: Schematics of WS-Module-rev1.3

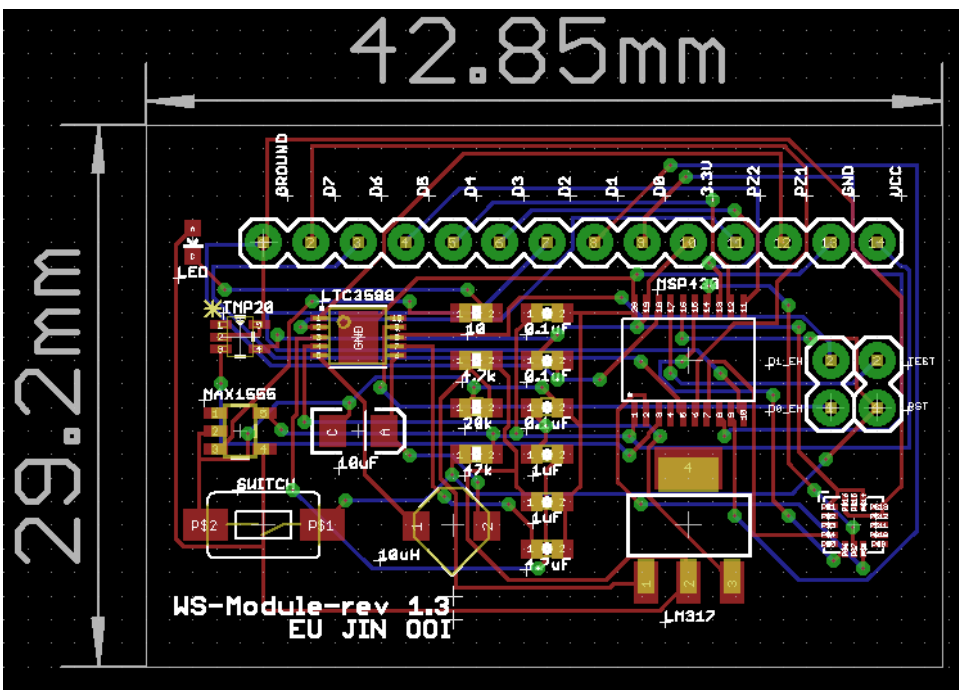

Figure 35: Board layout of WS-Module-rev1.3

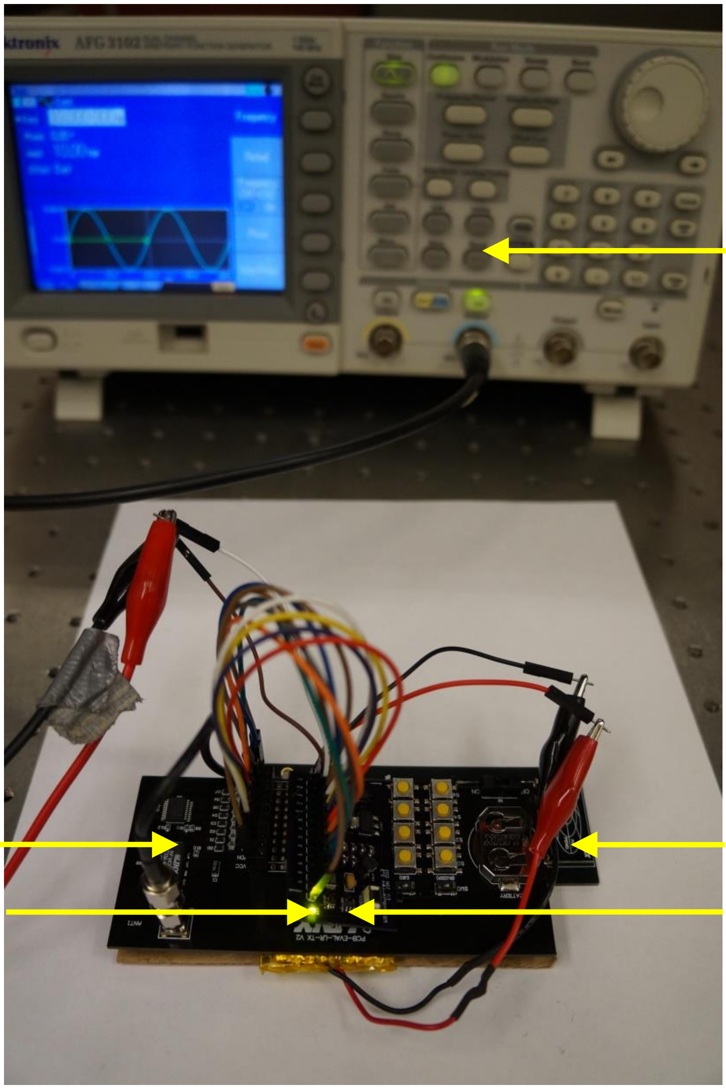

Figure 36: Populated WS-Module-rev1.3 connected to battery, radio module and AC source

4.3.5. WS-Module-rev1.4

WS-Module-rev1.4 integrates all the components in this design: microcontroller, sensors, radio module, energy conditioning and energy storage circuitry. The PCB is powered externally through a lithium-ion battery. Schematic of this design is shown in Figure 37 while the board layout is shown in Figure 38. Since this PCB was designed based on WS-Module Transmitter, it can be deduced that this design will not be functional due to the flaws in WS-Module Transmitter. However, this design demonstrates that this concept can be realized into a 50mm $\times$ 35mm PCB.

5. Summary and Future Work

In summary, a self-powered wireless sensor module is an idea which can be developed into reality. In this project, a microcontroller (MSP430G2553), a thermometer (TMP20), an accelerometer (ADXL362), a 433MHz radio transmitter (LR Series) and a PCB antenna (SP Series) are integrated into a 50mm $\times$ 35mm PCB. The circuit consumes 7.194μW on standby mode and 25.694mW on operational mode. This can be sustained by the current state-of-the-art piezoceramic energy harvester which is capable of generating 100μW from a body vibrating at a constant 1g or 9.81m/s^2 acceleration. This project serves as a proof of concept, and can be modified accordingly to requirements by using different electronic components.

If future work is to be carried out to this design, impedance matching to allow data transmission must be carried out, through proper PCB trace design. Range of data transmission should be tested to ensure it meets the theoretical 1km range. Packaging of the wireless sensor module must also be taken into account, and should be tested for robustness.

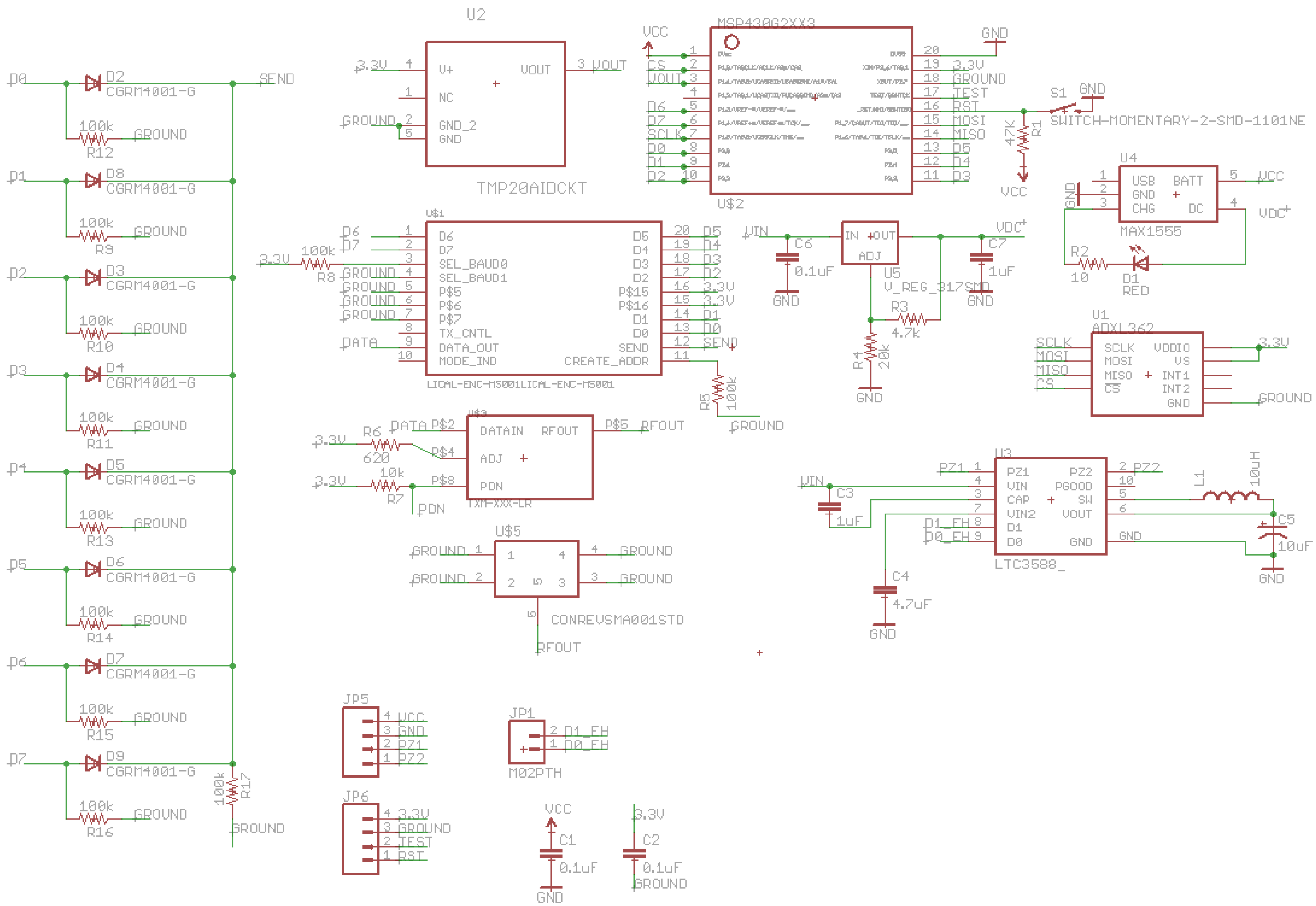

Figure 37: Schematics of WS-Module-rev1.4

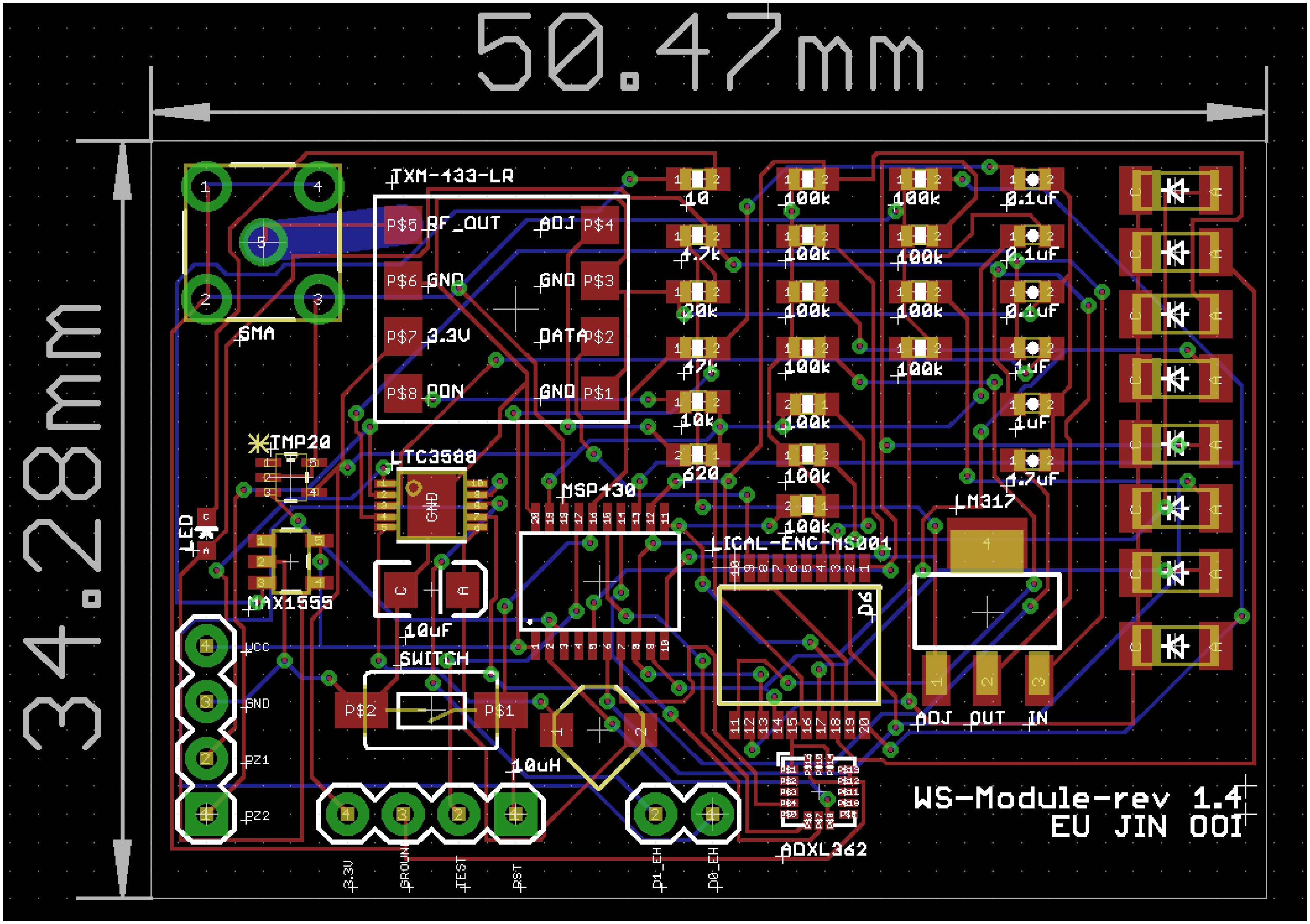

Figure 38: Board layout of WS-Module-rev1.4

6. References

[1] Arduino, "Arduino Uno," 2013. [Online]. Available: http://arduino.cc/en/Main/arduinoBoardUno. [Accessed 1 May 2013].

[2] Arduino, "Arduino Fio," 2013. [Online]. Available: http://arduino.cc/en/Main/ArduinoBoardFio. [Accessed 1 May 2013].

[3] Sparkfun Electronics, "Infrared Thermometer - MLX90614," 2013. [Online]. Available: https://www.sparkfun.com/products/9570. [Accessed 15 May 2013].

[4] Sparkfun Electronics, "Pulse Sensor," 2013. [Online]. Available: https://www.sparkfun.com/products/11574. [Accessed 15 May 2013].

[5] Texas Instruments, "MSP430 LaunchPad Value Line Development Kit," 2013. [Online]. Available: http://www.ti.com/tool/msp-exp430g2#0. [Accessed 1 June 2013].

[6] Sparkfun Electronics, "Triple Axis Accelerometer Breakout - ADXL362," 2013. [Online]. Available: https://www.sparkfun.com/products/11446. [Accessed 10 June 2013].

[7] Mouser Electronics, "Linx Technologies EVAL-433-LR," 2013. [Online]. Available: http://ca.mouser.com/ProductDetail/Linx-Technologies/EVAL-433-LR/?qs=K5ta8V%252bWhtZQ8bzSTCQmsg==. [Accessed 10 June 2013].

[8] R. Ben Mrad, Quantization Theory, A/D and D/A Conversions, Toronto, 2013.

[9] Texas Instrument, "Application Information," *Temperature Sensor (TMP20)*, vol. SBOS466, December, 2009.

[10] Linear Technology, "LTC3588 - Piezoelectric Energy Harvesting Power Supply," 2013. [Online]. Available: http://www.linear.com/product/LTC3588-1. [Accessed 25 July 2013].

[11] Sparkfun Electronics, "Energy Harvester - LTC3588 Breakout," 2013. [Online]. Available: https://www.sparkfun.com/products/9946. [Accessed 10 July 2013].

[12] Maxim Integrated, "MAX1551/MAX1555," *19-2902*, 2003.

[13] Electronics Lab, "LM317 Calculator," 2013. [Online]. Available: http://www.electronics-lab.com/articles/LM317/. [Accessed 1 August 2013].

[14] Fairchild Semiconductor, "LM317: 3-Terminal Positive Adjustable Regulator," 2013.

[15] Linx Technologies, "LR Series Basic Evaluation Kit," 2012. [Online]. Available: https://www.linxtechnologies.com/resources/data-guides/eval-xxx-lr.pdf. [Accessed 1 July 2013].

[16] OSH Park, "Pricing and Specifications," 2013. [Online]. Available: http://oshpark.com/pricing. [Accessed 22 July 2013].

[17] Missouri University of Science and Technology, "Microstrip Impedance Calculator," 2008. [Online]. Available: http://emclab.mst.edu/pcbtlc2/microstrip/. [Accessed 23 July 2013].

[18] Institute for Interconnecting and Packaging Electronic Circuits (Northbrook, Ill.), Institute for Interconnecting and Packaging Electronic Circuits (Evanston, Ill.). High Speed/High Frequency Committee. IPC-D-317 Task Group, Design Guidelines for Electronic Packaging Utilizing High-speed Techniques, IPC, 1995.